ABSTRACT SHEET, Paper Number 1224

Size Effects in Deformation and Fracture of a Ferritic Reactor Pressure Vessel Steel

T. Malmberg[(1)], K. Krompholz[(2)], D. Kalkhof[(2)], G. Solomos[(3)], E.C. Aifantis[(4, 5)]

(1) Forschungszentrum Karlsruhe GmbH, Institut für Reaktorsicherheit, Postfach 3640, D-76021 Karlsruhe, Germany
(2) Paul Scherrer Institut, Labor für Werkstoffverhalten, CH-5232 Villigen PSI, Switzerland
(3) European Commission, Joint Research Centre, Institute for Systems, Informatics and Safety, I-21020 Ispra/VA, Italy
(4) Aristotle University of Thessaloniki, Laboratory of Mechanics and Materials, GR-54006 Thessaloniki, Greece
(5) Michigan Technological University, Center for Mechanics of Materials and Instabilities, Houghton, MI 49931, USA

ABSTRACT

In support of small scale tests of reactor structures and to extend basic knowledge, screening material tests of different, geometrically similar specimens have been performed to examine the influence of size on the mechanical response. Among other nuclear steels and within the frame of the EU-project REVISA, the ferritic reactor pressure vessel steel 20MnMoNi55 was investigated under homogeneous and especially non-homogeneous states of strain and for quasi-static strain rate conditions both at room and elevated temperatures. The following tests have been performed:

- Tensile tests at room temperature (R.T.) and 400 °C of smooth and blunt-notched circular specimens (diameter: 3, 9, 30 mm) at two quasi-static strain rates
- Three-point bending at R.T. of U-notched beams (beam width: 10, 25, 140 mm) with scaled cross-head speeds, including detection of crack initiation with the D.C.-potential drop technique
- Tension creep of smooth circular specimens (diameter: 5 and 20 mm) under constant loads at different stress levels and temperatures enveloping the phase-transformation regime (700 °C, 800 °C, 900 °C).

All together 18 families of geometrically similar specimens were investigated and they have revealed size dependencies of various degrees. An influence of a macroscopic material heterogeneity (position effect) is present which impairs the interpretation of the results, especially of the smallest specimens; but it could be accounted for, at least in a qualitative sense, due to accompanying homogeneity assessment tests.

Some of the mayor trends are noted as follows. The smooth tension specimens, which are subjected to a macroscopic uniform strain distribution up to the maximum load, do not show a definite size-dependence. However, when necking sets in and a non-uniform strain distribution and damage are developing, the size dependence becomes apparent, e.g. the area reduction at fracture reduces with increasing size. The blunt-notched tension specimens do not show a definite size effect in the nominal stress-strain curves in the first part before the load maximum and also the values of the stress maxima are not affected. However, the stress maxima of the small specimens are clearly shifted to larger strains and the softening regimes are more extended.

On the contrary for the U-notched bending specimens almost the whole nominal stress-strain diagram, even before crack initiation, is affected with the tendency that smaller specimens are stronger than larger ones. Also crack initiation is more delayed the smaller the specimens. The volume-specific work for crack initiation was determined which consists of a size independent part and a part decaying with size.

The scaled creep tests revealed a strong dependence of the size influence on the stress and temperature level: size effects are largest at lower stress levels but the trend is depending on the temperature. At 700 °C and 900 °C the small specimens at the low stress level require much larger times to reach a given strain or rupture than large specimens; thus, predictions on this basis for large structures would be non-conservative. However, at 800 °C the reversed behavior is noted.

Clearly, further systematic research remains to be done to confirm the observed trends.

Size Effects in Deformation and Fracture of a Ferritic Reactor Pressure Vessel Steel

T. Malmberg[(1)], K. Krompholz[(2)], D. Kalkhof[(2)], G. Solomos[(3)], E.C. Aifantis[(4, 5)]

(1) Forschungszentrum Karlsruhe GmbH, Institut für Reaktorsicherheit, Postfach 3640, D-76021 Karlsruhe, Germany
(2) Paul Scherrer Institut, Labor für Werkstoffverhalten, CH-5232 Villigen PSI, Switzerland
(3) European Commission, Joint Research Centre, Institute for Systems, Informatics and Safety, I-21020 Ispra/VA, Italy
(4) Aristotle University of Thessaloniki, Laboratory of Mechanics and Materials, GR-54006 Thessaloniki, Greece
(5) Michigan Technological University, Center for Mechanics of Materials and Instabilities, Houghton, MI 49931, USA

ABSTRACT

In support of small scale tests of reactor structures and to improve and extend basic knowledge, screening material tests of different families of geometrically similar specimens have been performed to examine the influence of size on the mechanical response. Homogeneous and especially non-homogeneous states of strain at different temperatures and strain rates were considered, among other nuclear steels, for the ferritic reactor pressure vessel steel 20MnMoNi55. For this material the main results of quasi-static tensile tests of smooth and notched specimens at room and elevated temperature, as well as the results of quasi-static three-point bending tests of notched beam specimens at room temperature and creep tests of smooth specimens at high temperatures are presented and discussed.

1. INTRODUCTION

The question of similarity and non-similarity or size effects in deformation and failure is a long-standing problem but has gained recently considerable attention because of its importance for the transferability of mechanical test results of geometrically similar, scaled down structural models to the full scale structures using similitude laws (see Dolensky et al., division J, this conference). Moreover, it concerns also the validity of small scale laboratory type test results and their use as a basis for the computational modeling of large scale components. In support of small scale tests (e.g. scale 1:10) of reactor structures and to improve and extend basic knowledge, parts of the EU-project REVISA* are concerned with the size effect issue. Different families of geometrically similar specimens are used and screening material tests were performed up to failure to examine the influence of size on the mechanical response under homogeneous and especially non-homogeneous states of strain for different temperatures and strain rates for three different nuclear steels. This paper, however, is restricted to the investigation of the ferritic reactor pressure vessel steel 20MnMoNi55 (material no. 1.6310) under quasi-static strain rate conditions both at room and elevated temperatures. This ferritic steel, cast from a single heat, was delivered in form of eight plates (forged, 900 °C/water quenched, 730 °C, oven/air) with dimensions (1000 x 500 x 70 mm). The plates were certified according to KTA rules. The tests of families of geometrically similar specimens are broadly sketched as follows:

- Tensile tests at room temperature (R.T.) and 400 °C of smooth (R-type; Ref. [1]) and blunt-notched (T-type) circular specimens (diameter D_0: 3 mm, 9 mm, 30 mm; gauge length (uniform section)-to-diameter ratio 6). T-type specimens are provided with a circumferential semicircular notch at the center (notch radius R_0 = notch depth, R_0/D_0 = 1/10). The applied average strain rates are $2 \cdot 10^{-5}$ s^{-1} and 10^{-3} s^{-1} and refer to the uniform gauge length.
- Three-point bending tests at R.T. of U-notched (S-type; Ref. [2]) beams with rectangular cross-section (thickness B / width W / length L ratio 1/2/5.5; U-notch depth-to-width W ratio 1/5 and notch radius R-to-width W ratio 1/10; width W: 10, 25, 140 mm); testing with two sets of scaled cross-head speeds.
- Tension creep of smooth (C-type; Ref. [3]) circular specimens (diameter D_0: 5 and 20 mm, uniform gauge length-to-diameter ratio 5) under constant load at different stress levels and temperatures: (i) 700 °C, beginning of phase transformation regime (stress σ_0: 15, 25, 30 MPa), (ii) 800 °C, within the phase transformation regime (stress σ_0: 15, 25 MPa), (iii) 900 °C, beyond the phase transformation regime (stress σ_0: 10, 15, 25 MPa); preheated to reach isothermal conditions and tested in an inert atmosphere (flowing argon).

In addition, quasi-static and dynamic tensile test of smooth (Ref. [4]) and notched (Ref. [5]) specimens have been performed up to a strain rate of about 200 s^{-1} for this and other materials, however, with differently shaped tensile specimens (see also Solomos et al., division F, this conference). Furthermore, the REVISA-project included also a theoretical research task with the objective to exemplify the extend strain gradient plasticity captures the size influence on the deformation behavior (see Malmberg et al., division F, this conference).

* The financial support of the EU under the project "Reactor Vessel Integrity In Severe Accidents (REVISA)", contract F14S-CT96-0024, is gratefully acknowledged.

2. CUTTING PLANS, QUALITY ASSURANCE AND HOMOGENEITY ASSESSMENT

Detailed cutting plans were provided for the ferritic plates such that the specimens of different type and size were distributed over the plates, the larger specimens positioned at the mid-plane and the smaller ones also through the thickness (70 mm) of the plates. This included also standard tensile and Charpy impact specimens of one size to be used for quality assurance (QS) and homogeneity assessment. All specimens were oriented parallel to the long edges of the plates. The QS-specimens were positioned at the ends (position 01 and 03) and at the centers (position 02) of one diagonal of each plate. Of course, each specimen was properly marked to assure the identification of its origin (material, plate, position). Manufacturing reasons required that the small specimens (e.g. 3 mm ∅ tensile specimens) were grouped together in small sections of the plates. This generally implied that the smallest specimens were not positioned in the neighborhood of the largest ones.

The full program of the quality control and homogeneity assessment consisted of chemical analysis, metallography, Brinell-hardness tests as well as tensile and Charpy impact tests at R.T. and 300 °C. The following main results (Ref. [6]) were obtained for the ferritic steel 20MnMoNi55:

- The material satisfies the specifications.
- Neither from the standard chemical analysis, metallography, nor from hardness tests positional influences could be derived. However, metallographic investigations in the undeformed parts of used tensile specimens, done later in connection with fractographic investigations (Ref. [7]), revealed bands of brittle carbide segregations parallel to the long edges of the plates; the segregations appear to be typical for this steel.
- The tensile tests clearly revealed position dependent material properties within the plates and through their thicknesses, as well as from plate to plate. It was found that at room temperature position 01 of all plates (except plate 03) shows in the average a reduced (0.2%)-yield stress, increased ultimate stress and decreased area reduction at fracture as compared to positions 02 and 03 (position effect). For example, for plate 02 the corresponding percentage deviations are 15 % reduction of the yield stress, 6 % increase of the ultimate stress and 9 % reduction of the area reduction at fracture. This systematic inhomogeneity appears to be a consequence of the forging procedure. At 300 °C, however, this inhomogeneity is reduced; especially the area reduction becomes rather uniform. Therefore, special considerations are necessary, primarily at R.T., to account for pseudo-size effects and masking effects when the experimental results are interpreted.

3. EXPERIMENTAL RESULTS

3.1 Tensile Tests of Smooth Specimens

Before testing under non-uniform strain conditions is performed, the testing of smooth specimens with quasi-homogeneous strain distributions is necessary for checking to what extend size effects are present even under quasi-uniform strain distributions.

The measurements of the R1-, R2- and R3-specimens included: at R.T. the continuous measurement of the load, the deformation of the gauge length and the diameter change (also at the neck) using a video-extensometer; at 400 °C only the load and the gauge elongation could be measured by rods from outside the furnace; furthermore, after the tests were done, in all cases the broken halves of the specimens were joined and the gauge elongation, the minimum diameter at neck and radius of curvature of the meridional contour of the neck at the minimum cross-section were determined.

Investigations of first results obtained at R.T. and at a strain rate of 10^{-3} s^{-1} (Ref. [8]) revealed a somewhat increased ultimate strength of the smallest specimens as compared to the largest ones. This effect could be identified as a pseudo-size-effect due to positional influences on the tensile characteristics (Ref. [8]). These early investigations and the additional results at low strain rates ($2 \cdot 10^{-5}$ s^{-1}) and higher temperatures (400 °C) allow the following main conclusions for the R-type specimens (Ref. [1]): (i) The ultimate stress and the uniform elongation are essentially size independent. (ii) The hardening is similar up to the ultimate stress but deviations and size effect trends occur when necking sets in. (iii) Whereas the fracture elongation does not show a consistent trend when the size is increased from 3 to 30 mm ∅, the local strain measure "reduction of area" shows no or a slight decrease with diameter change from 3 to 9 mm but an increase from 3 to 30 mm ∅ yields a relative decrease of the area reduction of at most 8 % at R.T.; at 400 °C, the relative decrease is about 15 %. (iv) The normalized radius of curvature R/D_0 of the meridional neck contour shows a non-monotonous (first increase then decrease) size dependence for both strain rates and temperatures. Generally, however, the lowest values are found for the largest specimens. (v) Generally, cup and cone fracture was found for the smallest specimens at both strain rates and temperatures. But for the largest specimen R3 at R.T. a milling cutter type fracture was observed, which appears to be induced by the carbide segregations. However, at 400 °C the cup and cone type fracture was restored (Ref. [1, 7]).

In qualitative terms the experimental findings agree with observations reported in the literature (Ref. [9]). An exception is, however, the non-monotonous size dependence of the normalized meridional radius of curvature which disagrees with previous observations (monotonic increase with size, Ref. [8, 9]).

3.2 Tensile Tests of Blunt-Notched Circular Specimens

For the T-type specimens under quasi-static conditions at R.T. continuous measurements of the load, the gauge elongation, the diameter change at the root of the notch and the notch opening using a video-extensometer were performed. At 400 °C continuous measurements of the notch deformation could not be made. Of course, after fracture the gauge elongation and the notch deformations (minimum diameter, notch opening and radius of curvature of the meridional notch profile) were recorded by joining the broken halves.

A large part of the small T1-specimen originate from position 01 of plate 02. Consequently, the associated material inhomogeneity has to be accounted for when experimental results are interpreted. The following observations and conclusions for the T-type specimens were obtained.

The diagrams of the nominal stress (engineering stress at the root of the notch) versus the nominal strain (average strain in the gauge section) show an overlapping scatter in the whole strain range of the medium and large specimens (type T2 and T3) at R.T. and 400 °C and for both strain rates ($2 \cdot 10^{-5}$ and 10^{-3} s^{-1}). However, small T1-specimens yield a larger maximum nominal stress and a softening regime which differs markedly from that of the large specimens. Since the small specimens come from position 01, they have a somewhat increased strength; therefore the increase of the maximum stress can be interpreted as a pseudo-size effect. However, the shift of the stress maximum of the small T1-specimens to larger strains and their larger softening regimes reflect a size effect, which at R.T. is possibly even partially masked by the reduced ductility of these specimens.

The nominal stress versus two strain measures at the notch, namely the diametrical strain and the relative notch opening measured at R.T. only, show similar trends but, as expected, even more pronounced size influences with a definite order (Figs. 1 & 2); the small T1-specimens yield the most extended softening range whereas the ranges of the medium size and larger size specimen are successively decreased. The difference between the strains at the lowest comparable stress level of the small and the largest specimens amounts up to a factor of 2. The shift of the maximum of the nominal stress to larger global and local strain motivates the suggestion that softening inducing damage processes, occurring before the maximum load and leading to crack extension, are size dependent. However, no steps were taken to detect crack initiation.

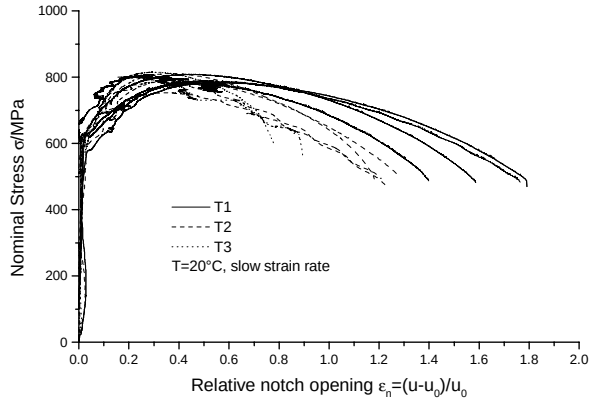

Fig. 1: Nominal stress versus relative notch opening; notched tensile specimens

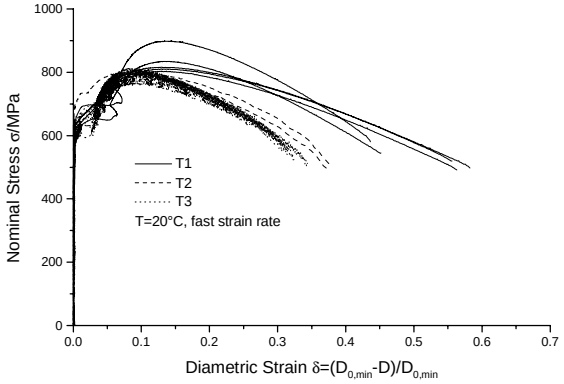

Fig. 2: Nominal stress versus diametric strain at root of the notch; notched tensile specimens

The local notch deformations were determined also after fracture for all specimens. It is noted that the endpoints of the continuous measurements during the tests do not necessarily agree with the measurements at the broken specimens. This investigation reveals that the local variables of the small T1-specimens tested at R.T. accumulate around two different mean values (Fig. 3). They are mainly related to two sets of small specimens which come from two adjacent sections about 50 mm apart at position 01 of plate 02. The results at 400 °C do not show this scatter of the small specimens since they come only from one section and since heterogeneities are partially equalized.

At R.T. (Fig. 3) and also at 400 °C (Fig. 4) the diametric strain and the correlated area reduction show an approximately linear decay with size if the small, less ductile specimens are excluded in Fig. 3. If all test results at R.T. of the small specimens are included, then the size dependence at R.T. flattens out in the range of small specimens in Fig. 3.

The mean value of the relative notch opening at R.T is relatively insensitive to a change in size. However, at 400 °C (Fig. 5), where positional effects are less important for the small specimens, the small T1-specimens yield an average relative notch opening which is more than 1.8 times larger than those of the medium and the large size specimens which do not show a difference (Fig. 5). This rather steep decay of the size dependence of small specimens has not been observed for the other local strain measures. Also the temperature rise from R.T. to 400 °C has only a moderate influence on the medium and large size specimens but a significant influence on the smaller specimens.

Another representative measure of the notch deformation is the radius of curvature R of the meridional contour of the notch. Its determination, which is a somewhat subtle procedure, revealed that in all cases a segment of a circle could be laid into the notch after fracture. At R.T. the normalized radius of curvature $R/D_{0\,min}$ ($D_{0\,min}$: minimum initial diameter at the root of the notch) is relatively insensitive to a change in size. However, at 400 °C (Fig. 6) there is almost no difference between the small and the medium size specimens whereas the large specimens yield considerably reduced normalized radii for both quasi-static strain rates.

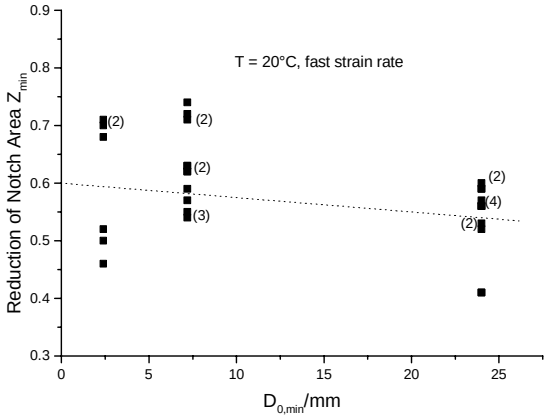

Fig. 3: Area reduction at notch after fracture versus minimum initial notch diameter at R.T.; notched tensile specimens

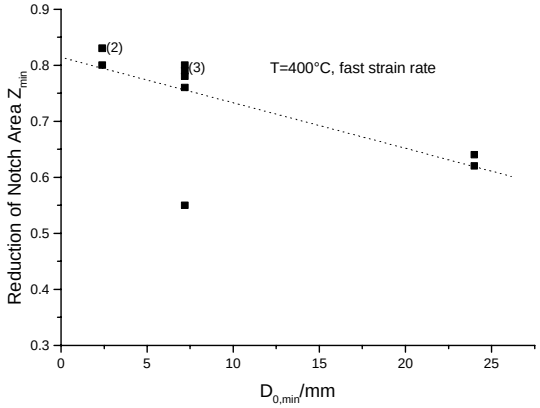

Fig. 4: Area reduction at notch after fracture versus minimum initial notch diameter at 400 °C; notched tensile specimens

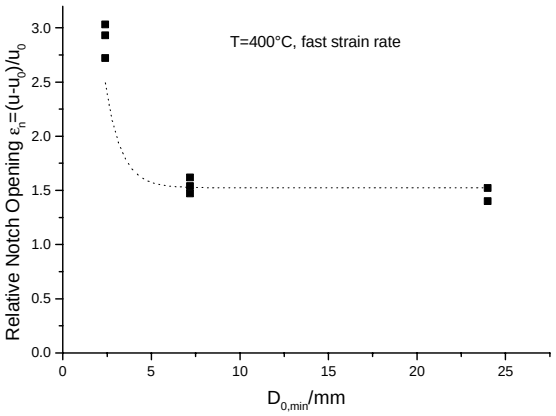

Fig. 5: Relative notch opening at fracture versus minimum initial notch diameter at 400 °C; notched tensile specimens

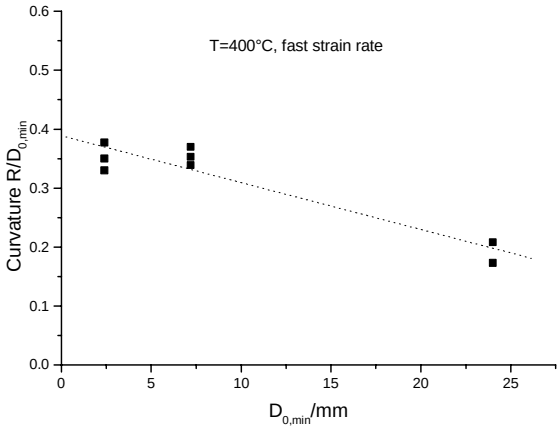

Fig. 6: Normalized radius of curvature of the meridional notch contour versus minimum initial notch diameter at 400 °C; notched tensile specimens

3.3 Quasi-Static Three-Point Bending of U-Notched Beam Specimens

The tests of the S1-, S2 and S3-specimens were performed with scaled supports (span = 4 x W) at R.T. up to some instant beyond the maximum load but without complete fracture (Ref. [2]). The cross-head velocities were scaled such that the nominal strain rate at the root of the notch remained the same. Apart from the load, the load-point displacement and the notch opening were recorded with a video-extensometer and crack initiation was detected by the D.C.-potential drop technique. Also the crack extension at termination of the experiment was determined by heat tinting and subsequent fracture at liquid nitrogen temperature.

Diagrams of the normalized load (normalized with respect to the limit load) versus the normalized load-point displacement (normalized with respect to the width W) as well as representations of the nominal stress (load divided by the ligament area) versus the relative notch opening (Figs. 7 & 8) were generated which essentially yield the same general trends. This is due to the fact that the beam deflection is primarily controlled by the notch deformation. Figs. 7 & 8, related to different sets of scaled cross-head speeds, show that the scatter bands are well separated except for the very first part: in the elastic regime and for very small plastic deformations with displacements less than about 5 % of the width W of the beam all results are within a single scatter band. This implies that the classical geometric scaling applies

within this regime (Ref. [10]). Beyond this and even before the indicated crack initiation, the results for the three different sizes are clearly separated such that for a given normalized load-point displacement or relative notch opening the small specimens yield the largest normalized load or nominal stress which reduces successively for the medium and large size specimens. The maxima follow the same order, a decay function with increasing size. The maxima of the largest specimens amount only about 70 % of that of the smallest.

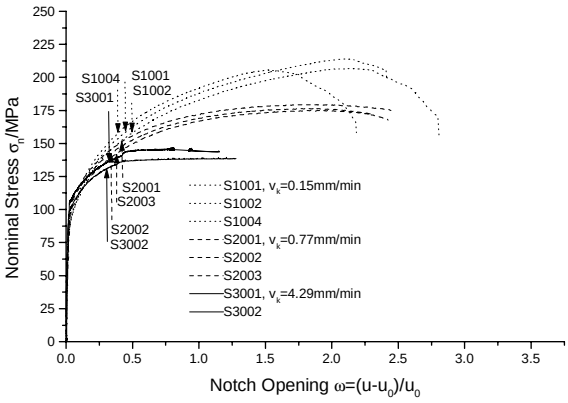

Fig. 7: Nominal stress versus relative notch opening; indication of crack initiation; notched bending specimens at R.T., fast scaled cross-head speeds

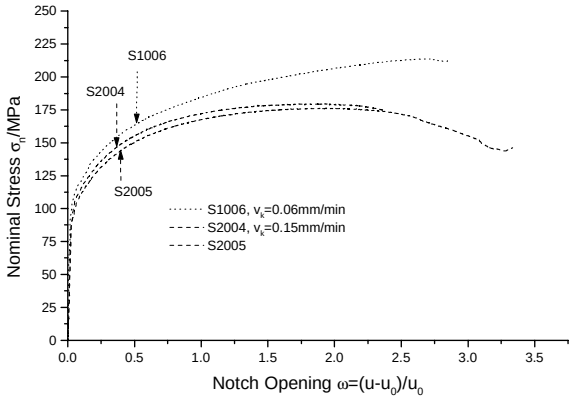

Fig. 8: Nominal stress versus relative notch opening; indication of crack initiation; notched bending specimens at R.T., slow scaled cross-head speeds

The relative notch openings corresponding to the stress maxima show a considerable scatter for the small S1-specimens which are subjected to a positional influence (reduced ductility); it is expected that this suppresses their deformation ability (masking effect). Nevertheless, the mean values obey the following sequence: the small specimens yield the largest load-point displacements or relative notch openings, the medium size specimen somewhat smaller values and the large size distinctly smaller values. The results for the scaled slow speed tests (Fig. 8), however, show a more pronounced order for the S1- and S2-specimens since these specimens are not affected by a position effect.

For the instant of crack initiation the small S1-specimens require larger critical normalized displacements and relative notch openings than the medium size S2-specimens and the critical values for the large S3-specimens are the smallest (see arrow markers in Figs. 7 & 8)). However, the differences between these critical values are relatively small.

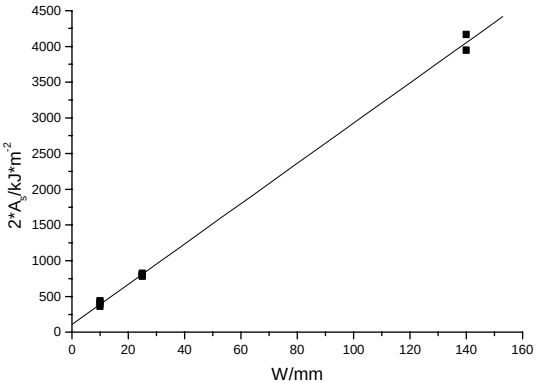

Fig. 9: Area specific work for crack initiation versus beam width; notched bending specimens at R.T., slow and fast tests

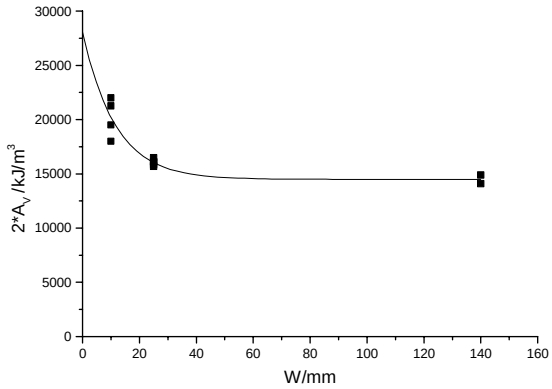

Fig. 10: Volume specific work for crack initiation versus beam width; notched bending specimens at R.T., slow and fast tests

The required work for crack initiation was obtained by integrating the load-displacement curves up to the instant of crack initiation. Referring it to the corresponding ligament area, yields the area specific work A_s which is shown in Fig. 9 as a function of the specimen size. It is noteworthy that it increases linearly with the characteristic dimension, the width of the beam, with a non-zero extrapolated value for very small specimens. Dividing the area specific work by the width of the notch, the required work A_v for crack initiation and per active notch volume is obtained. This volume specific work is shown in Fig. 10. It is non-linearly decaying with size and it consists of two terms: (i) a size dependent hyperbolic decay term analogous to the size dependent initiation of crack extension in fracture mechanics and (ii) a size independent

constant term corresponding to the classical size independent plasticity. For the smallest specimens tested (type S1, notch radius 1 mm) the first term amounts about 28 % of the total volume specific work. The volume specific work A_v for crack initiation is caused by two size dependent contributions: (i) the increase of the normalized load for a given normalized displacement with decreasing size before crack initiation; this size dependence of the normalized load-displacement curves or nominal stress-relative notch opening diagrams has not been observed for the blunt-notched tension specimens; it is possibly induced by the highly non-uniform strain field in front of the notch where the non-uniformity due to bending and due to the notch effect are combined. Then the size dependence of the response may possibly be related to a size dependence of the plastic material behavior (e.g. gradient effects), but certainly also due to a size dependence of the damage phenomena which lead to crack generation. (ii) Furthermore, the shift of the instant of crack initiation to larger normalized displacements or relative notch openings with decreasing size.

Inspection of the fractured specimens showed that the onset of crack growth occurred in the mid-thickness of the specimen in all cases. At a very late state the cracks were visible at the flanks at the specimen notches. Generally, a variety of micro-cracks were visible at the notch root from which the main crack started.

3.4 Tension Creep of Smooth Specimens

During the creep tests the elongation of the gauge length was continuously recorded up to failure by an inductive extensometer adapted to rods outside of the furnace within a chamber. After fracture the elongation of the gauge length and the area reduction at the fractured neck were determined. This was supplemented by metallographic investigations. Prior to creep testing, the temperature and time dependence of the scale oxidation and the temperature regime of the phase transformation were determined.

Creep curves "strain versus time" for the small C1- and the large C2-specimens were obtained for the various stress levels and at the three temperatures. A characteristic result is shown in Fig. 11. Depending on the stress level, a considerable size influence is observed. To quantify the trends several characteristic creep data were determined: the times $t_{5\%}$, $t_{15\%}$ and t_f to 5 % and 15 % strain and to rupture, the minimum (secondary) creep rate dε/dt, the elongation A_u and area reduction Z_u after rupture. The corresponding data are listed in Tab. I. The following observations and conclusions are obtained (Ref. [3]).

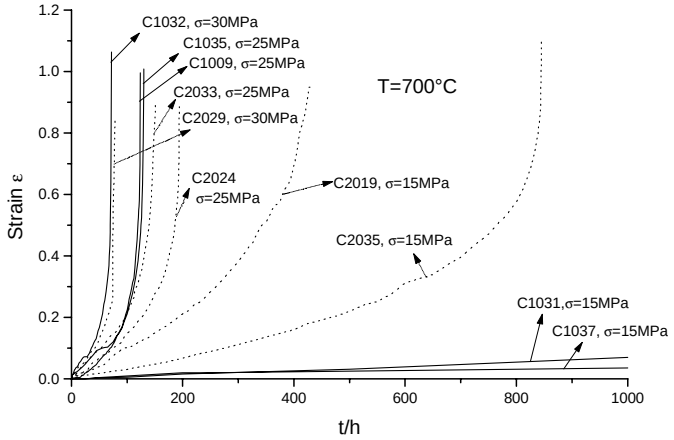

Fig. 11: Total strain versus time: creep specimens C1, C2 (5, 20 mm∅), 700 °C

The size dependence of the times to 5 % and 15 % strain and to rupture show the same tendencies for a given stress and temperature level. The effect is largest at 700 °C and at the lowest stress level (15 MPa), i.e. the times to 5 % and 15 % strain are 10 and 6 times longer for the small C1-specimen than for the large C2-specimen (Tab. I); rupture did not yet occur for the small specimens after 2800 h whereas the large C2-specimens failed below 900 h. At 700 °C with increasing stress the magnitude of the size effect decreases and at the highest stress level (30 MPa) a reversal of the effect may occur. At 900 °C a similar but much less pronounced trend is observed. Thus, at these temperatures and low stress levels predictions of critical times on this basis for large structures would be non-conservative. At 800 °C the size effect is again largest at the lowest stress (15 MPa, factor of 5 and 6 in the times) and it decreases with increasing stress. However, the effect is reversed, i.e. small specimens yield considerably shorter times in the whole stress range (15 – 25 MPa).

It is generally observed that the trend of the size influence on the times to a given strain or to rupture is also reflected in the minimum creep rate since large rates correspond to small times. At 700 °C the elongation and the area reduction at rupture are not available for the small C1-specimens at the lowest stress level since the specimens did not fail yet. At 800 °C and 900 °C the elongation at rupture of the small C1-specimens are larger than that of the large C2-specimens at all stress levels, but to a varying degree (Tab. I). The largest effect is found for the lowest stress level (factor of 2) and this

trend is also reflected by the area reduction. If the temperature dependence of the creep ductility measures "elongation and area reduction" are considered, then a minimum is found between 800 °C and 900 °C, independent of the stresses in the range 15 – 25 MPa, which is likely related to the co-existence of the ferritic and austenitic phases.

Tab. I: Creep data for small C1- und large C2-specimens

Specimen	T/°C	σ_0/MPa	$t_{5\%}$/h	$t_{15\%}$/h	t_f/h	$d\varepsilon/dt*10^3$/h	A_u	Z_u
C1001	900	25	2.7	5.2	8.5	49.8	0.94	0.64
C2001			1.0	3.7	9.4	51.4	0.71	0.58
C1002	900	15	6.7	20.5	74.9	7.24	0.96	0.72
C1036			8.3	24.3	56.5	7.35	0.66	0.51
C2003			8.0	26.1	53.5	5.57	0.60	0.52
C2034			8.3	23.3	52.0	6.76	0.59	0.56
C1003	900	10	31.0	127.1	444.4	0.98	1.26	0.97
C2002			17.5	78.0	222.3	2.03	0.60	0.56
C1034	800	25	7.2	15.3	20.0	25.9	0.70	0.51
C1005*			4.5	11.3	23.0	15.8	0.38	0.66
C1004*			-	-	22.5	-	0.3	0.62
C2031			13.0	42.0	82.0	3.59	0.71	0.51
C2020			6.8	27.0	41.7	5.07	0.56	0.54
C2021			9.8	41.0	84.5	3.33	0.74	0.58
C1008*	800	15	35.5	67.3	78.6	2.00	0.25	0.71
C1033			14.5	36.4	62.0	4.66	0.66	0.68
C2022*			110.0	242.0	357.2	0.59	0.39	0.54
C2030			164.0	370.0	494.0	0.46	0.35	0.41
C1032	700	30	13.2	47.0	72.0	2.31	1.06	0.97
C2029			21.0	54.5	78.0	2.45	0.84	0.96
C1035	700	25	44.8	85.7	139.3	1.87	1.01	0.88
C1009			25.3	86.0	123.9	1.91	1.00	0.93
C2024			35.2	101.0	194.0	1.68	0.84	0.97
C2033			24.7	75.5	151.2	3.04	0.90	0.96
C1031	700	15	544.0	1630.0**	>1437	0.092	-	-
C1037			1720	-	>2800	0.049	-	-
C2019			62.0	150.0	427.0	1.22	0.95	0.95
C2035			162.0	380.0	845.0	0.485	1.10	0.96

* Specimens fractured outside the gauge length. ** Estimated value. Shadowed fields: Specimens from position (01).

It is quite obvious that the size effect trends observed at one temperature may not be transferred to another one even qualitatively. Different micro-structural properties at the three test temperatures are present due to the phase transformation from the ferritic α-phase to the austenitic γ-phase which was determined to be in the temperature range from 690 °C to 840 °C. Furthermore, metallographic investigations of specimens subjected to creep at 700 °C indicate a larger content of the austenitic phase than inspected from the law of balance. This gives rise to the suggestions that the mechanical stress may affect the phase transformation.

It was found that the macroscopic material inhomogeneity can be excluded as a primary cause for the observed size influences since the main size effects are much larger than the positional influence on the creep data. Also orientation effects as well as severe oxidation cannot serve as explanations since all specimens have the same orientation in the plates and testing was done in an inert atmosphere. It suggests itself that some diffusional process may be responsible since diffusional processes are more important in small specimens then in large ones. Thus, if sufficient time is available, such processes become important and size influences due to diffusion may show up. Since creep tests at lower stress levels have longer duration than at higher stresses, diffusional induced size effects should be more pronounced at low stress levels. This, in fact, has been observed, but still considerable assessment is required.

4. CONCLUSIONS

Four specimen types, produced from the ferritic reactor pressure vessel steel 20MnMoNi55, were investigated under various test conditions (all together 18 families of geometrically similar specimens of R-, T-, S-. and C-type) and they have revealed size dependencies of various degrees. An influence of the macroscopic material heterogeneity (position

effect) is present for the smallest specimens but it could be accounted for, at least in a qualitative sense, due to the extensive homogeneity assessment testing. Under quasi-static conditions the nominal stress-strain diagrams of the smooth and the blunt-notched tensile specimen (R- and T-type) as well as those of the three-point bending tests of the U-notched beam specimens (S-type) appear to show a certain trend on a phenomenological level: the smooth R-type specimens, which are subjected to a macroscopic uniform strain distribution up to the maximum load, do not yield a size dependence when the position effect is properly accounted for. However, when necking sets in and a non-uniform strain distribution and damage are developing, the size dependence becomes apparent, e.g. the area reduction at fracture reduces with increasing size. The blunt-notched T-type specimens under tension do not show a definite size effect in the nominal stress-strain curves in the first part before the maximum and also in the values of the stress maxima if the position effect is taken into consideration. However, the stress maxima of the small specimens are definitely shifted to larger strains and their softening regimes are much more extended; also a size dependent order of the softening part is observed with the tendency that, for a given stress level, smaller specimens yield larger deformations. Whereas for these specimen types the size influence apparently does not affect the first part of the nominal stress-strain curves, for the S-type bending specimens almost the whole nominal stress-strain diagram, even before crack initiation, is affected with the tendency that smaller specimen are "stronger" than larger ones. Also crack initiation is shifted to larger strains when the size is decreased. Only the elastic and a range of small plastic strain appears to be size invariant. It is conjectured that the high non-uniformity of the strain at the root of the notch due to the combined bending and the notch effect produces this behavior. Evidently, it is important for the understanding to determine the whole nominal stress-strain (preferably "local" strains) diagrams and not only stress maxima and quantities after fracture. Since the propagation of a macroscopic crack induces size effects, it is necessary to determine the initiation of cracks. Because of the difficulty to realize this, independent approaches are recommended.

The scaled creep tests with the C-type specimens have revealed a strong dependence of the size influence on the stress and temperature level around the phase transformation regime: size effects are largest at low stress levels but the trend is depending on the temperature: whereas at 700 °C and 900 °C the small C1-type specimens at the low stress level require much larger times than the large C2-type specimens to reach a given strain or rupture ("non-conservative" behavior), at 800 °C the reversed behavior is found. Thus, the obtained creep results are in conflict with the statement of the ASTM designation E139 that size influences can be neglected provided the material is sound and is not subjected to appreciable corrosion or orientation effects, conditions which do not apply in the creep tests outlined above.

Considerable systematic research remains to be done to confirm the observed trends by investigating more homogeneous materials, using improved cutting plans, extending the size and temperature range and studying other specimen types. Some of these studies are part of the ongoing EU-project LISSAC (see Krieg et al., division P, this conference).

REFERENCES

[1] Krompholz, K., Kamber, J., Groth, E., Kalkhof, D., "Size effect studies on smooth tensile specimens at room temperature and 400 °C", *Paul Scherrer Institut, PSI-Report No. 00-02*, June 2000

[2] Krompholz, K. Groth, E., Kalkhof, D., "Size effect studies on geometrically scaled three point bend type specimens with U-notches", *Paul Scherrer Institut, PSI-Report No. 01-03*, March 2001

[3] Krompholz, K. Groth, E., Kalkhof, D., "Size effect studies of the creep behavior of 20MnMoNi55 at temperature from 700 °C to 900 °C", *Paul Scherrer Institut, PSI-Report No. 00-07*, Nov. 2000

[4] Solomos, G., Albertini, C., Labibes, K., Pizzinato, V., et al., "Experimental investigations of strain rate, temperature and size effects in nuclear steels (smooth specimens)", *European Commission, Joint Research Centre Ispra, Technical Note No. I.00.76*, June 2000

[5] Solomos, G., Albertini, C., Labibes, K., Pizzinato, V., et al., "Experimental investigations of size effects in nuclear steels using notched tensile specimens", *European Commission, Joint Research Centre Ispra, Technical Note No. I.00.136*, November 2000

[6] Krompholz, K., Kamber, J., Kalkhof, D., "A preliminary study of material homogeneity for size effect investigations", *Paul Scherrer Institut, PSI-Report No. 9903*, June 1999

[7] Materna-Morris, E., "Investigations of size and strain rate influences on fracture surfaces of smooth tensile specimens of austenitic and ferritic steels X6CrNb1810 and 20MnMoNi55", *Forschungszentrum Karlsruhe, Scientific Report FZKA 6525*, publication in preparation

[8] Malmberg, T., Krompholz, K., Solomos, G., Aifantis, E.C., "Investigations on size effects in ferritic and austenitic materials", *Trans. 15th Int. Conf. Structural Mechanics in Reactor Technology (SMiRT-15)*, Seoul, Korea, Aug. 15-20, 1999, paper L06/5

[9] Malmberg, T., Tsagrakis, I., Eleftheriadis, I., Aifantis, E.C., "On the gradient plasticity approach to size effects, Part I: Reviews", *Forschungszentrum Karlsruhe, Scientific Report FZKA 6321*, March 2001

[10] Malmberg, T., "Aspects of similitude theory in solid mechanics, Part I: Deformation behavior", *Forschungszentrum Karlsruhe, Scientific Report FZKA 5657*, Dec. 1995